1040-5488/14/9109-0000/0 VOL. 91, NO. 9, PP. 00–00
OPTOMETRY AND VISION SCIENCE

ORIGINAL ARTICLE

Comparative Study of Lens Solutions Ability to Remove Tear Constituents

Steven Cheung*, Holly Lorentz†, Elizabeth Drolle*, Zoya Leonenko‡, and Lyndon W. Jones§

ABSTRACT

Purpose. The purpose of this study was to use atomic force microscopy to compare and characterize the cleaning abilities of a hydrogen peroxide–based system (HPS) and a polyhexamethylene biguanide–containing multipurpose solution (MPS) at removing *in vitro* deposited tear film constituents, as well as to determine deposition patterns on various silicone hydrogel contact lenses.

Methods. Silicone hydrogel materials—balafilcon A (BA), lotrafilcon B (LB), and senofilcon A (SA)—were incubated for 1 week in an artificial tear solution (ATS) containing representative lipids, proteins, and salts from the tear film. Atomic force microscopy was used to resolve each lens before and after being cleaned overnight in HPS or MPS. Atomic force microscopy was used again to resolve HPS/MPS-cleaned lenses, which were reincubated in fresh ATS for 1 week, before and after an overnight clean in their respective cleaning solution.

Results. Atomic force microscopy imaging was able to characterize lens deposits with high resolution. Lenses incubated in ATS revealed distinct differences in their deposition pattern across lens materials. The surface of BA contained about 20-nm-high deposits, whereas deposit heights up to 150 nm completely occluded the surface of SA. Lotrafilcon B lenses revealed clusters of deposits up to 90 nm. The use of either lens solution left trace amounts of tear film constituents, although components from the MPS were seen adsorbed onto the surface after cleaning. Surface roughness (R_a) measurements revealed a significant difference between ATS-incubated and HPS/MPS-cleaned SA and LB lenses ($p < 0.05$). R_a between first incubated and HPS/MPS-cleaned reincubated SA and LB was also significant ($p < 0.05$).

Conclusions. Unique variations in ATS deposition patterns were seen between lenses with atomic force microscopy. The application of both HPS and MPS removed most visible surface deposits.

(Optom Vis Sci 2014;91:00–00)

Key Words: silicone hydrogel contact lens, tear film, deposition, atomic force microscopy, cleaning solution

Silicone hydrogel (SH) lenses have become increasingly popular, as eye care practitioners are choosing to prescribe them over conventional lenses[1] owing to their superior oxygen permeability compared with hydrogel lenses.[2–4] The advent of SH lenses in the late 1990s addressed this issue of hypoxia, particularly during overnight wear, by incorporating siloxane components into conventional hydrogel materials, thus making the lens highly oxygen transmissible.[5–7]

As with any material in contact with a biological system, all contact lenses have a tendency to sorb components from the surrounding tear film, specifically proteins and lipids, and the deposition profiles of hydrogel and SH materials differ.[8] The hydrophobic siloxane component results in SH lenses sorbing a higher amount of lipids than hydrogel lenses.[9–11] Protein deposition also occurs on SH lenses, but the degree of protein deposition is less than that seen on hydrogel lenses,[12–15] and the protein that does deposit appears to be largely denatured.[15–17] Furthermore, the presence of these deposits disrupts the smooth lens surface and may contribute to symptoms of dryness and discomfort.[18,19]

To improve wettability and minimize the deposition of proteins and lipids, some SH lenses require surface modifications.[6] One example is a surface treatment known as plasma oxidation that is seen in balafilcon A (BA) (PureVision) lenses, where hydrophilic silicate compounds are formed on the lens surface by transforming the original siloxane inside a reactive gas chamber.[20] On a microscopic scale, discontinuous, glassy silicate islands are present at the surface and macropores are seen to extend into the material.[21,22] In

*BSc
†PhD, FAAO
‡PhD
§PhD, FCOptom, FAAO
Centre for Contact Lens Research, School of Optometry and Vision Science (SC, HL, LWJ), Department of Biology (ED, ZL, LWJ), and Department of Physics and Astronomy (ZL, LWJ), University of Waterloo, Waterloo, Ontario, Canada.

TABLE 1.
Contact lens care solution characteristics

Brand	Manufacturer	Disinfecting agent	Other agents	Buffer
ClearCare	Alcon Vision Care (Fort Worth, TX)	3% H_2O_2	Pluronic 17R4	Phosphate
SoloCare Aqua	Menicon (Nagoya, Japan)	Polyhexamethylene biguanide 0.0001%	Dexpanthenol, sorbitol, sodium phosphate, Pluronic F127 (poloxamer 407), 0.025% ethylenediamine tetraacetic acid (EDTA)	Tris

comparison, lotrafilcon B (LB) (Air Optix Aqua) lenses are subjected to a different surface treatment, called plasma polymerization. These lenses enter a gas reactive plasma chamber containing a mixture of trimethylsilane oxygen and methane that envelops the lens in a 25-nm continuous film of cross-linked hydrocarbons containing hydrophilic groups.[23] This process results in a very smooth, continuous coating that entirely covers the underlying lens material.[22,24] Unlike BA and LB lenses, the surface of senofilcon A (SA) (Acuvue OASYS) lenses is not plasma treated. Instead, these lenses have polyvinylpyrrolidone (PVP) interspersed as an internal wetting agent to increase the overall wettability of the lens,[25] resulting in a surface that appears very different to that seen with either BA or LB.[22] Understanding these specific contact lens modifications, how they are created, how they alter the contact lens surface and how tear film components and disinfecting solutions interact with the altered surfaces is imperative for researchers and practitioners to identify the best combination of lens and cleaning solution for lens wearers.

Patients who remove and then reinsert their lenses need an appropriate care regimen to clean and disinfect their lenses. The two most common types of cleaning and disinfecting solutions available today are nonpreserved hydrogen peroxide–based systems (HPSs) and preserved multipurpose solutions (MPSs).[1,26] Modern-day cleaning solutions incorporate a variety of surfactants and wetting agents to help remove surface deposits and increase the overall wettability of the lens by lowering the surface tension.[27,28] A major difference between these two solution systems is that most MPSs include a manual rubbing and/or rinsing step before overnight soaking,[29,30] whereas HPSs typically eliminate this step to maximize convenience for patients. Although literature on the efficacy of rub/no-rub cleaning products is scarce, the few papers that do address this issue consistently report that including a rub step provides enhanced removal of deposits, bacteria and debris from the lens.[31–36]

Atomic force microscopy (AFM) is a powerful tool to characterize the topography of sample surfaces with high nanometer and subnanometer resolution, and its application in vision science has been steadily increasing over the past 15 years.[37] In AFM, a microscale cantilever with a 10- to 15-μm-sized tip at its end is used to scan the surface and resolve the surface morphology. As the tip scans the surface, forces between the tip and sample change and cause the cantilever to deflect. These deflections are registered and are used to produce a three-dimensional image of surface morphology.[37] Several studies have used AFM to characterize surface features of both conventional and SH lenses,[22,24,38–45] although none have used it to investigate the cleaning abilities of care regimens.

The primary purpose of this *in vitro* study was to use AFM to evaluate different combinations of cleaning solutions (HPS and MPS) onto three different SH contact lenses. The cleaning efficacy and potential process of removing deposits from an artificial tear solution (ATS) will be examined. In addition, the deposits onto the lens surface will also be characterized using AFM.

METHODS

An HPS (ClearCare; Alcon Vision Care, Fort Worth, TX) and a polyhexamethylene biguanide–containing MPS (SoloCare Aqua; Menicon, Nagoya, Japan) were investigated (Table 1). Their cleaning abilities and long-term effects on different SH materials were studied after being incubated in an ATS, using AFM. Experiments involving HPS and MPS were conducted *in vitro* and independently from each other, although they were performed in parallel to identify any differences in cleaning ability (Fig. 1).

Three SH materials were examined: BA (PureVision; Bausch & Lomb, Rochester, NY), LB (Air Optix Aqua; Alcon Vision Care, Fortworth, TX), and SA (Acuvue OASYS; Johnson & Johnson, Jacksonville, FL). The physical and chemical properties of these materials are found in Table 2. All lenses were unworn, with a spherical power of −3.00 diopters (D) and a base curvature of about 8.6 ± 0.2 mm.

Artificial Tear Solution

The protocol for the ATS preparation has been previously published and can be referred to for more detail.[46,47] Table 3 shows the protein and lipid composition of the ATS along with the ingredients of the complex salt solution (CSS), which was used as a base for the ATS. However, this current study differed somewhat in that it did not involve radioactively labeled components and two proteins (bovine

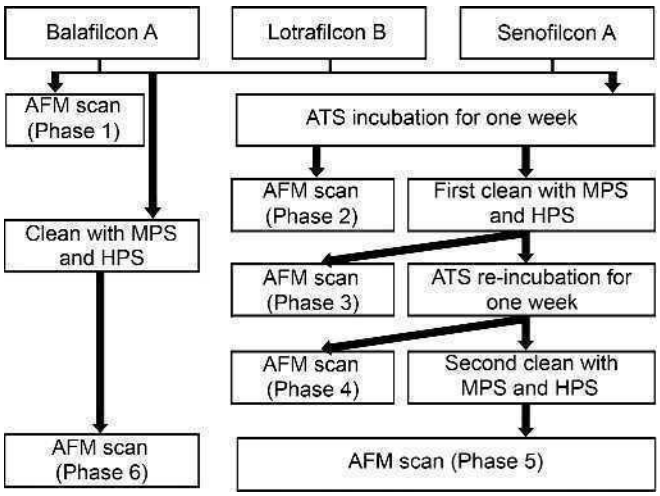

FIGURE 1.
Experimental outline depicting layout of cleaning study involving HPS and MPS.

TABLE 2.
Physical and chemical properties of SH lens material

USAN	Balafilcon A	Lotrafilcon B	Senofilcon A
Proprietary name	PureVision	Air Optix	Acuvue OASYS
Manufacturer	Bausch & Lomb	Alcon Vision Care	Johnson & Johnson
Power, D	−3.00	−3.00	−3.00
Base curvature, mm	8.6	8.6	8.4
Diameter, mm	14.0	14.2	14.0
Water content, %	36	33	38
Surface treatment	Plasma oxidation	Plasma polymerization (25 nm plasma coating)	Internal wetting agent (PVP)
FDA group	V	V	V
Ionicity	Ionic	Nonionic	Nonionic
Principal monomers	NVP + TPVC + NVA + PBVC	DMA + TRIS + siloxane monomer	mPDMS + DMA + HEMA + siloxane macromer + TEGDMA + PVP

DMA, *N*,*N*-dimethylacrylamide; HEMA, poly-2-hydroxyethyl methacrylate; mPDMS, monofunctional polydimethylsiloxane; NVA, *N*-vinyl aminobutyric acid; NVP, *N*-vinyl-pyrrolidone; PBVC, poly(dimethysiloxy)di(silybutanol)bis(vinyl carbamate); TEGDMA, tetraethyleneglycol dimethacrylate; TPVC, tris-(trimethylsiloxysilyl)propylvinyl carbamate; TRIS, trimethylsiloxy silane; USAN, United States adopted name.

immunoglobulin G and bovine colostrum lactoferrin) were excluded because of cost considerations.

Pretreatment of Vials

Previous work undertaken at the Centre for Contact Lens Research (unpublished) has revealed that up to 80% of lipids in the ATS adsorbs onto the interior surface of the glass vials used during the deposition incubation process. Therefore, it is imperative to pretreat the vials with ATS so that the concentrations of proteins and lipids in the final ATS remain constant. For this study, 20-mL glass scintillation vials were pretreated with 6 mL of ATS for at least 4 days at 37°C on a rotary shaker. Afterward, the used ATS was removed, the vials were rinsed with saline, and 6 mL of fresh ATS was added.

ATS Incubation of Contact Lenses

Each lens was removed from its blister package with sterile silicone-tipped forceps and rinsed with CSS. Lenses were placed in a 12-well plate, where each lens was immersed in 5 mL of CSS for 24 to 48 hours on a rotary shaker at room temperature. This

TABLE 3.
Artificial tear solution components

Complex salt solution component	Molecular formula	Concentration, mM
Sodium chloride	NaCl	90.0
Potassium chloride	KCl	16.0
Sodium citrate	$Na_3C_6H_5O_7$	1.5
Glucose	$C_6H_{12}O_6$	0.2
Urea	$(NH_2)_2CO$	1.2
Calcium chloride	$CaCl_2$	0.5
Sodium carbonate	Na_2CO_3	12.0
Potassium hydrogen carbonate	$KHCO_3$	3.0
Sodium phosphate dibasic	Na_2HPO_4	24.0
Hydrochloric acid (10 M)	HCl	26.0
ProClin 300 (Supelco 48912-U)	—	0.2 mL/L
MilliQ Water	H_2O	—
Protein component	**Molecular weight, kDa**	**Concentration, mg/mL**
Bovine albumin	66.4	0.20
Hen egg lysozyme	14.3	1.90
Bovine submaxillary mucin	3 × 105 to 4 × 107	0.15
Lipid component	**Molecular formula**	**Concentration, mg/mL**
Triolein	$C_{57}H_{104}O_6$	0.016
Cholesterol	$C_{27}H_{46}O$	0.0018
Oleic acid	$C_{18}H_{34}O_2$	0.0018
Oleic acid methyl ester	$C_{19}H_{36}O_2$	0.012
Cholesteryl oleate	$C_{45}H_{78}O_2$	0.024
Phosphatidylcholine	$C_{42}H_{82}NO_8P$	0.0005

procedure is designed to remove any blister solution residues present on the lens so that it does not interfere with lens incubation in the ATS.

Once the lenses had been presoaked in CSS, they were individually added to pretreated scintillation vials containing 6 mL of fresh ATS, sealed with Parafilm, and incubated at 37°C on a rotary shaker for 1 week. A total of 60 lenses were investigated in this study. Twenty lenses of each lens material (BA, LB, or SA) were incubated and divided into two groups to study the effects of MPS and HPS on each lens type (Fig. 1).

Atomic Force Microscopy

Contact lens samples were imaged in air using a JPK Nanowizard II AFM (JPK Instruments, Berlin, Germany). Nanoworld pyramidal NCH (Neuchâtel, Switzerland) cantilevers with 42 N/m spring constant and resonance frequency of about 320 kHz were used to image the samples in intermittent contact mode. To scan the curved contact lenses, a spherical glass stand was created to maintain curvature of the sample while scanning.

Three representative 10- by 10-μm AFM scans were taken and analyzed from each lens phase duplicate (n = 2) at the center to characterize surface morphology. Each lens was removed from its vial or lens case with sterile, blunt metal tweezers and was placed in the center of the spherical glass stand and air dried for 5 minutes. This served to secure the lens onto the spherical glass to minimize artifacts that may be produced during the imaging process.

Phase 1: Blister Control

A control lens for each material was scanned with AFM directly upon removal from their blister package. These served as a baseline comparison when examining against treated lenses.

Phase 2: ATS Incubation

Lenses that had been incubating in ATS for 1 week were scanned with AFM.

Phase 3: First Clean

Lenses that were incubated in ATS were cleaned overnight with HPS/MPS by following the instructions found on the product. After overnight exposure to the HPS or MPS, each lens material was scanned with AFM the next morning.

Phase 4: ATS Reincubation

HPS/MPS-cleaned lenses were reincubated in fresh ATS for 1 week at 37°C on a rotary shaker in their same pretreated vial. After the incubation period, lenses were scanned with AFM.

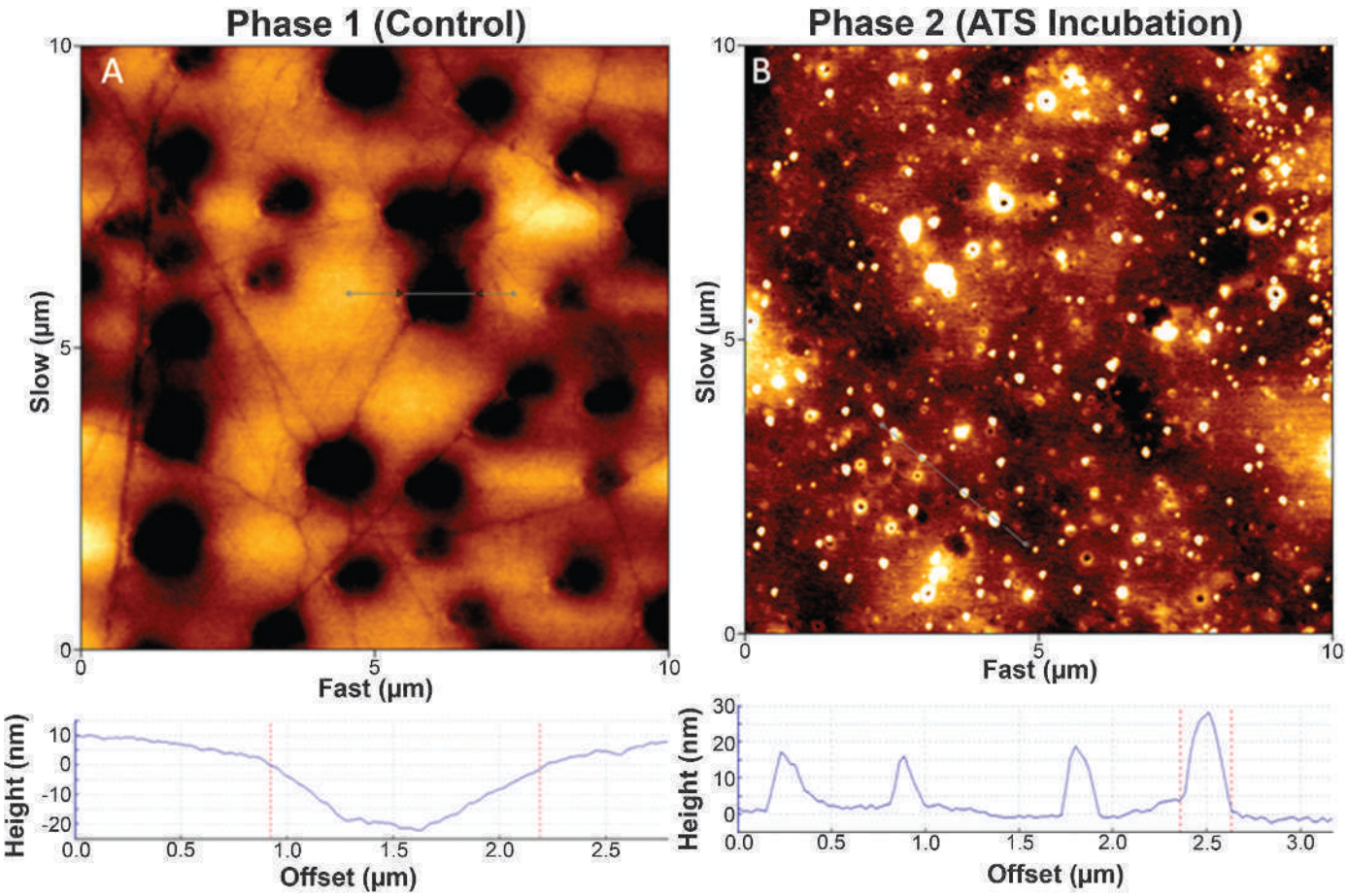

FIGURE 2.

Surface topography of BA before cleaning. Images were obtained using AFM. Beneath each image is its associated cross section displaying relative heights. (A) Control lens surface out of its blister package. (B) Lens surface after incubating in ATS for 1 week.

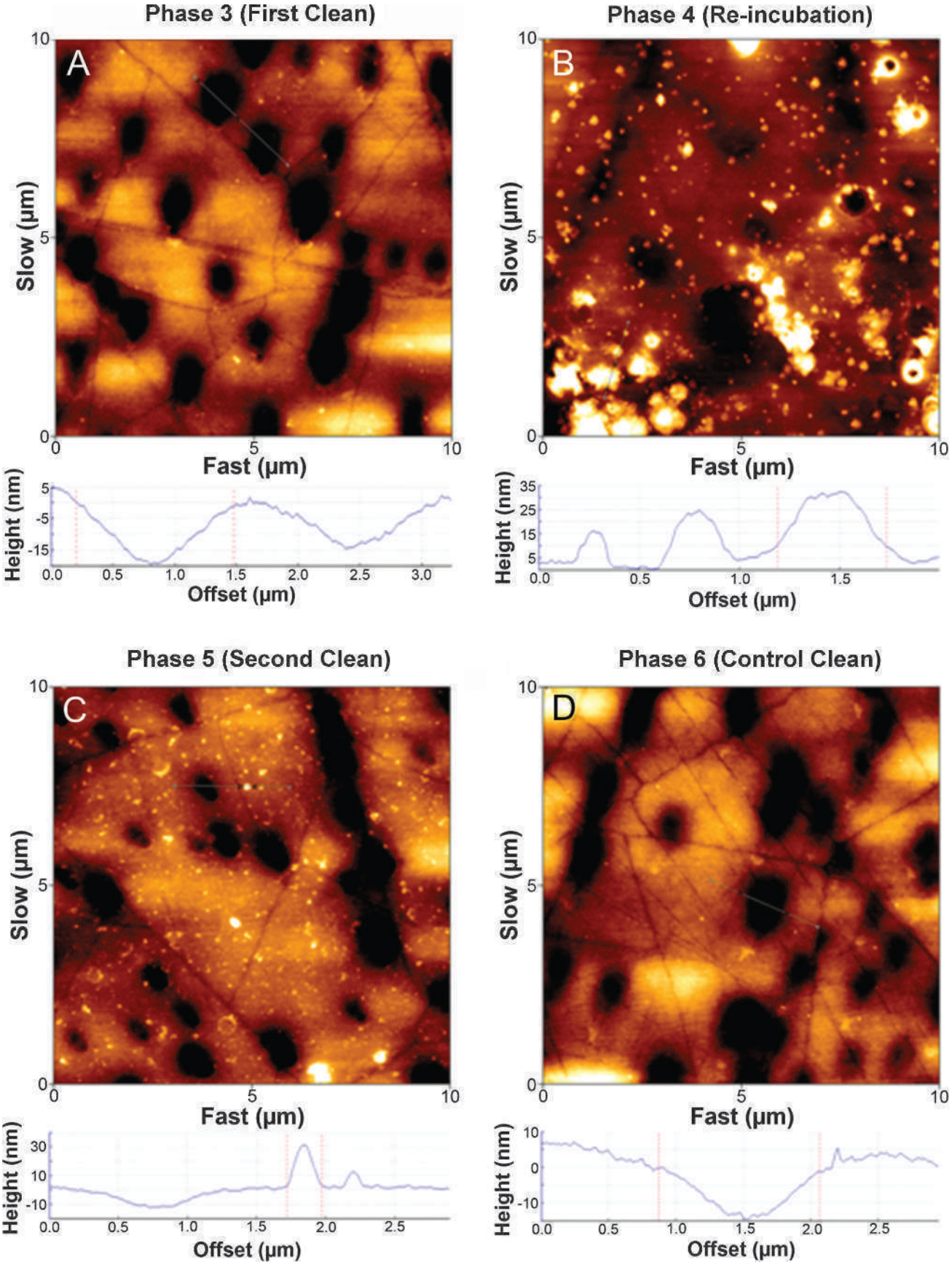

FIGURE 3.

Surface topography and cross section of BA with HPS cleaning. Images were obtained using AFM. Beneath each image is its associated cross section displaying relative heights. (A) Lens surface after first overnight clean with HPS. (B) HPS-cleaned lens surface after reincubating in ATS for 1 week. (C) Lens surface after second overnight clean with HPS. (D) Control lens surface cleaned with HPS.

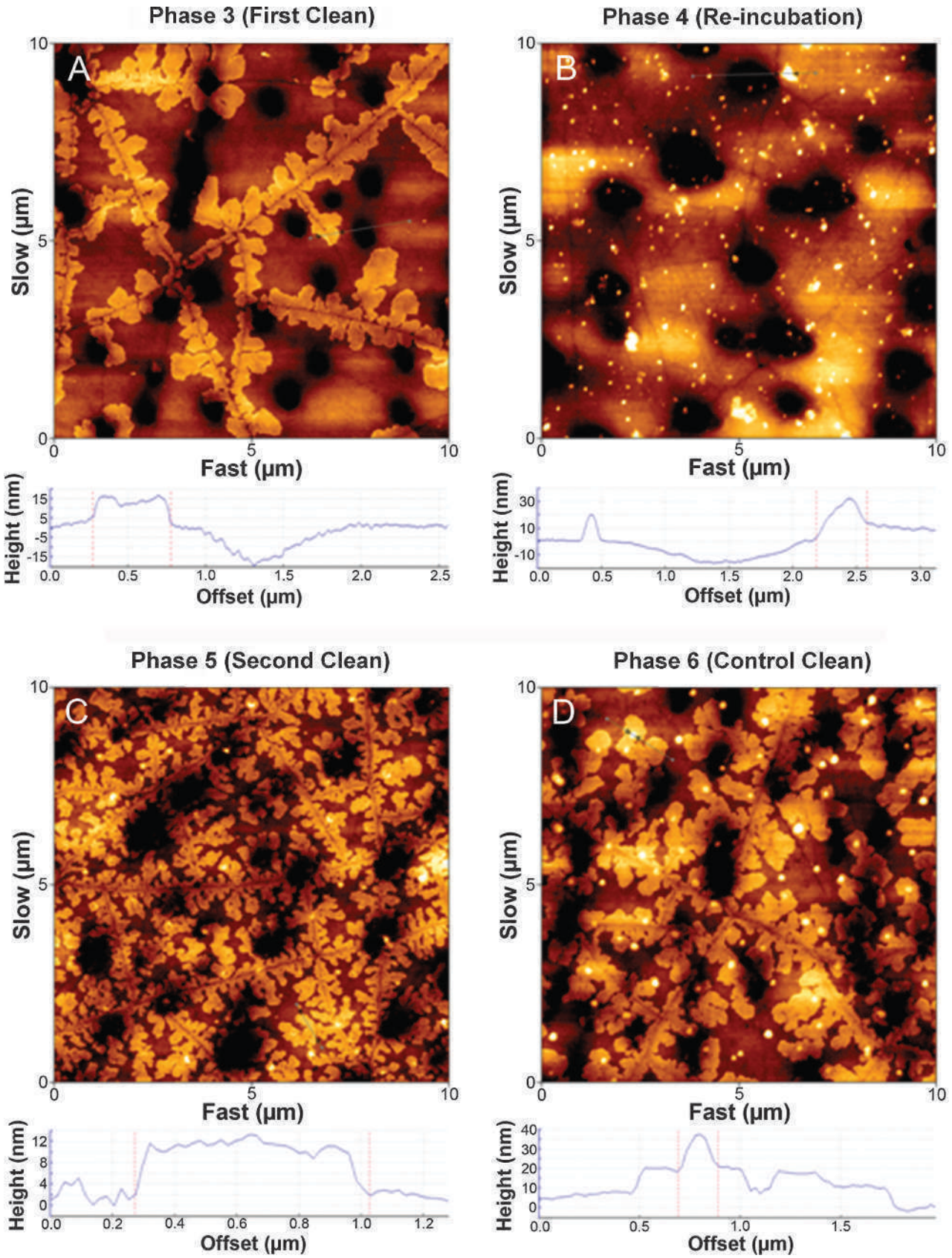

FIGURE 4.

Surface topography and cross section of BA with MPS cleaning. Images were obtained using AFM. Beneath each image is its associated cross section displaying relative heights. (A) Lens surface after first overnight clean with MPS. (B) MPS-cleaned lens surface after reincubating in ATS for 1 week. (C) Lens surface after second overnight clean with MPS. (D) Control lens surface cleaned with MPS.

Phase 5: Second Clean

Lenses that were reincubated in ATS were cleaned overnight for the second time with their respective cleaning solution and then scanned the next morning.

Phase 6: Control Clean

A control clean for each lens was scanned with AFM to determine the effect HPS and MPS have on the material without the presence of the ATS constituents. Lenses were rinsed with CSS, as described above, and cleaned overnight with HPS and MPS. Atomic force microscopy scans were taken the following morning.

AFM Image Processing and Surface Roughness

Atomic force microscopy topography images were processed and flattened with the JPK data processing software. A cross section was made through the highest feature on each image to determine its relative height. The average surface roughness (R_a) for each phase duplicate was obtained by taking 10 random cross sections from six AFM scans and calculating the average R_a.

Statistical Analysis

Statistical analysis was conducted using Statistica 10 (StatSoft Inc, Tulsa, OK). A repeated-measures analysis of variance was used to compare the R_a of phase 2 with phase 3 and phase 4 lenses. Factors included in the analysis of variance were contact lens material, cleaning solution, and time point. The Tukey Honestly Significant Difference test was used for *post hoc* comparisons, where $p < 0.05$ was considered significant.

RESULTS

Balafilcon A, LB, and SA lens materials were investigated for their interaction with an ATS by examining their surface topography using AFM. After 1 week of incubation in ATS, each of the three lens surfaces yielded a distinct appearance in terms of deposition height, location, and density.

The results will be described in terms of phases of the study, as previously mentioned. Phase 1, blister control; phase 2, ATS incubation; phase 3, first clean; phase 4, ATS reincubation; phase 5, second clean; phase 6, control clean.

Balafilcon A

A 10- by 10-μm AFM scan of BA in phase 1 (A) and 2 (B) is shown in Fig. 2. In phase 1, a relatively flat surface is seen with its discontinuous silicate islands and about 20-nm-deep macropores, which is evident in the cross-sectional view below the scan. In comparison, phase 2 contained deposits adsorbed uniformly across the surface with an average height of 20 nm. Additionally,

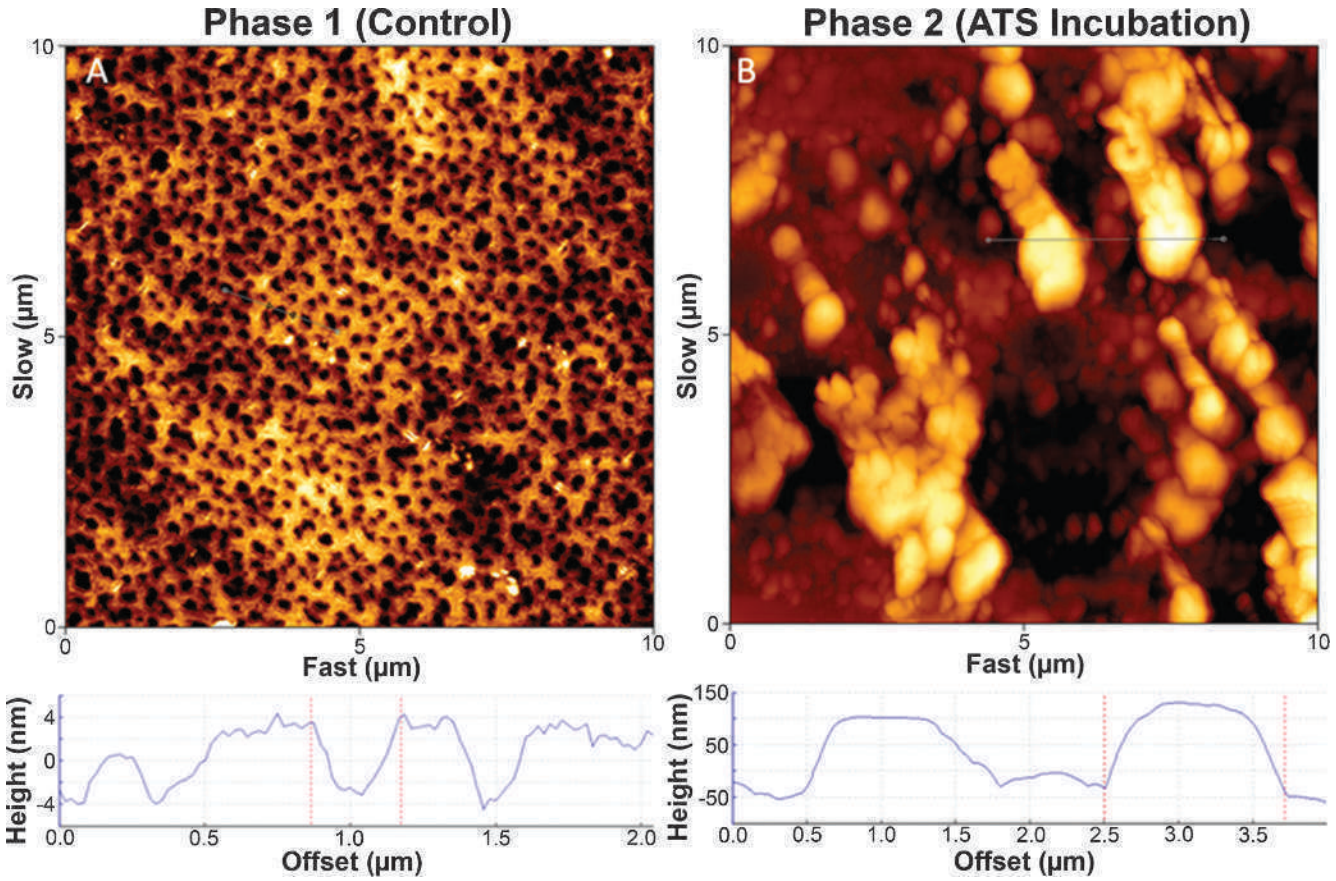

FIGURE 5.

Surface topography and cross section of SA before cleaning. Images were obtained using AFM. Beneath each image is its associated cross section displaying relative heights. (A) Control lens surface out of its blister package. (B) Lens surface after incubating in ATS for 1 week.

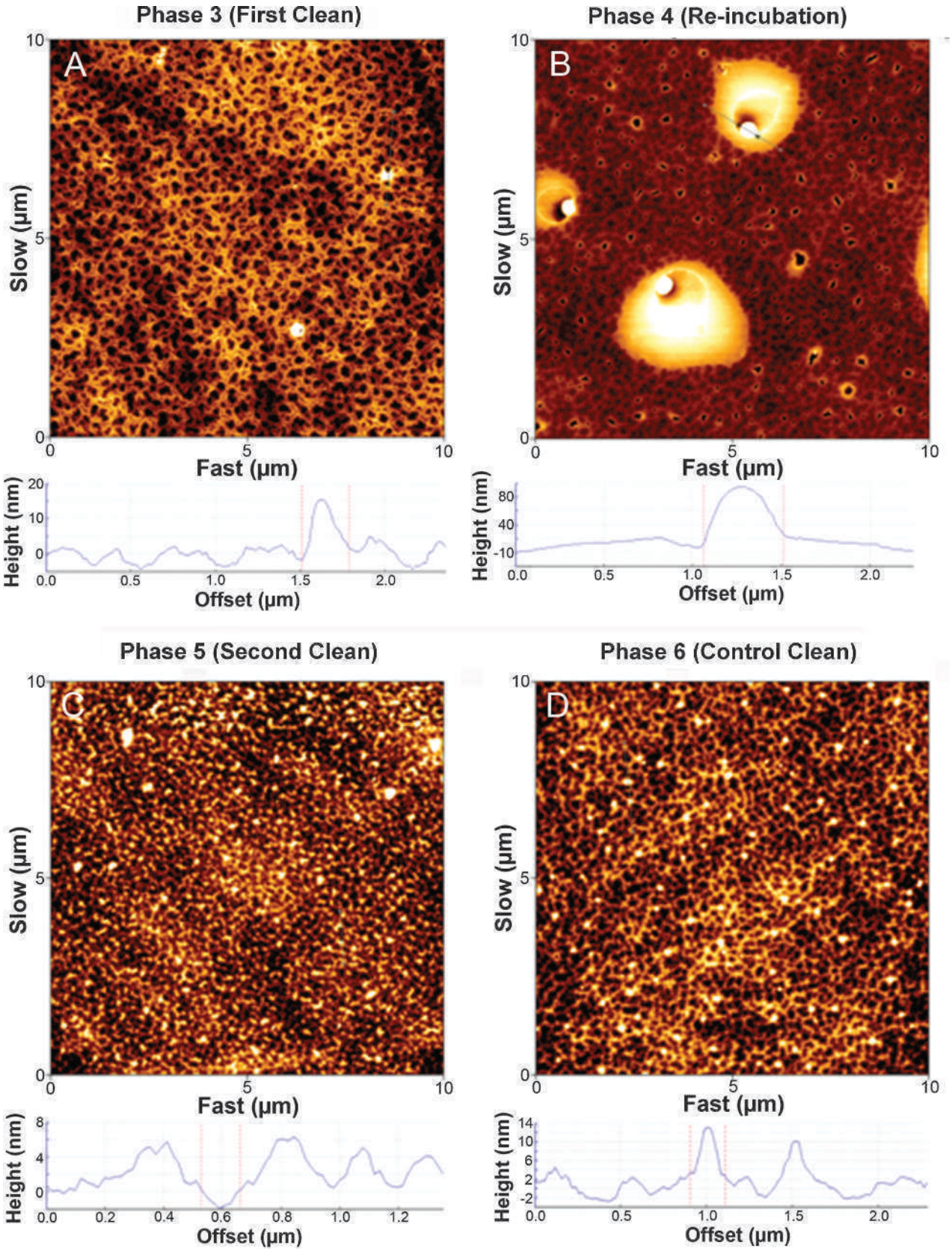

FIGURE 6.

Surface topography and cross section of SA with HPS cleaning. Images were obtained using AFM. Beneath each image is its associated cross section displaying relative heights. (A) Lens surface after first overnight clean with HPS. (B) HPS-cleaned lens surface after reincubating in ATS for 1 week. (C) Lens surface after second overnight clean with HPS. (D) Control lens surface cleaned with HPS.

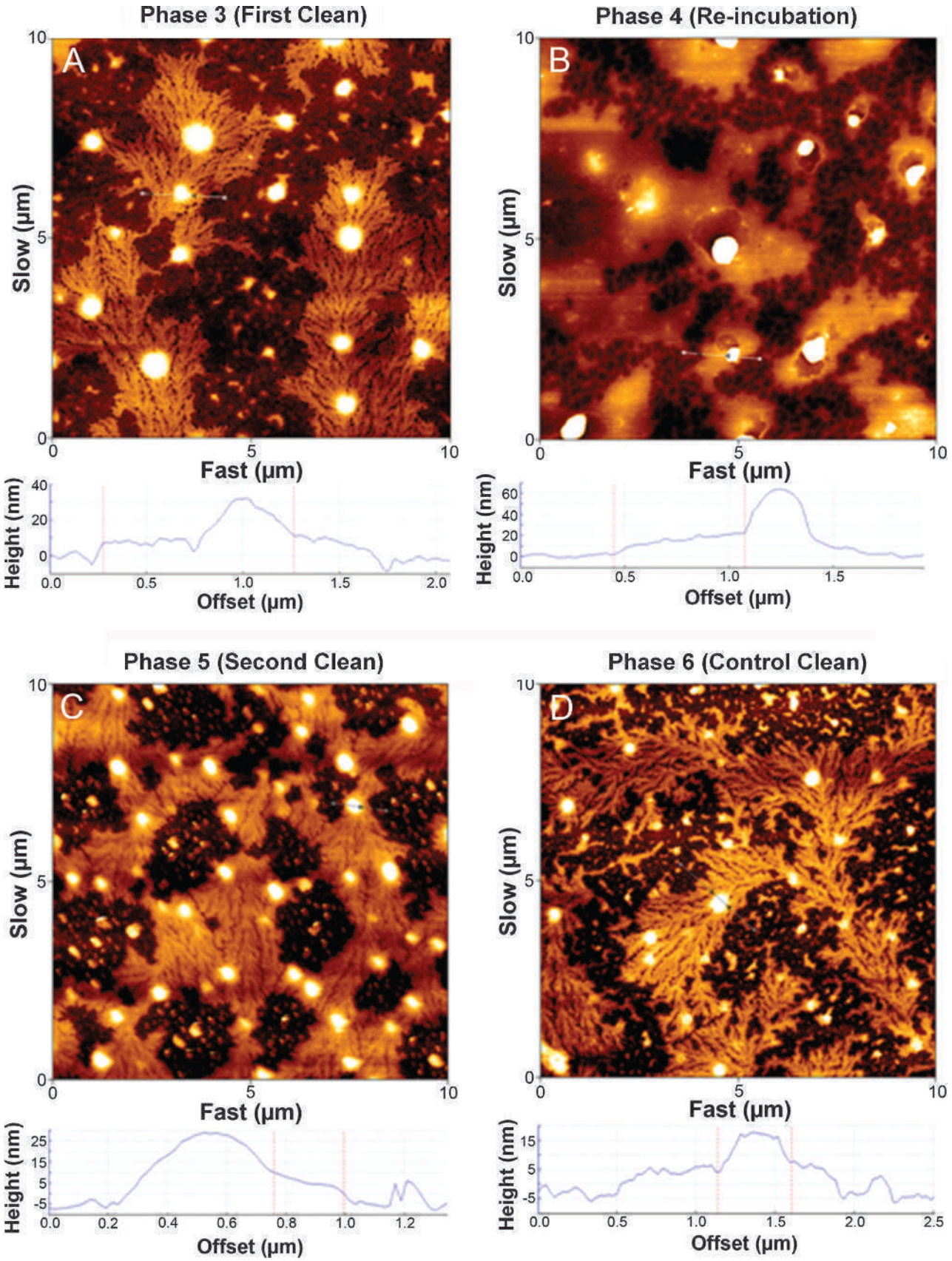

FIGURE 7.

Surface topography and cross section of SA with MPS cleaning. Images were obtained using AFM. Beneath each image is its associated cross section displaying relative heights. (A) Lens surface after first overnight clean with MPS. (B) MPS-cleaned lens surface after reincubating in ATS for 1 week. (C) Lens surface after second overnight clean with MPS. (D) Control lens surface cleaned with MPS.

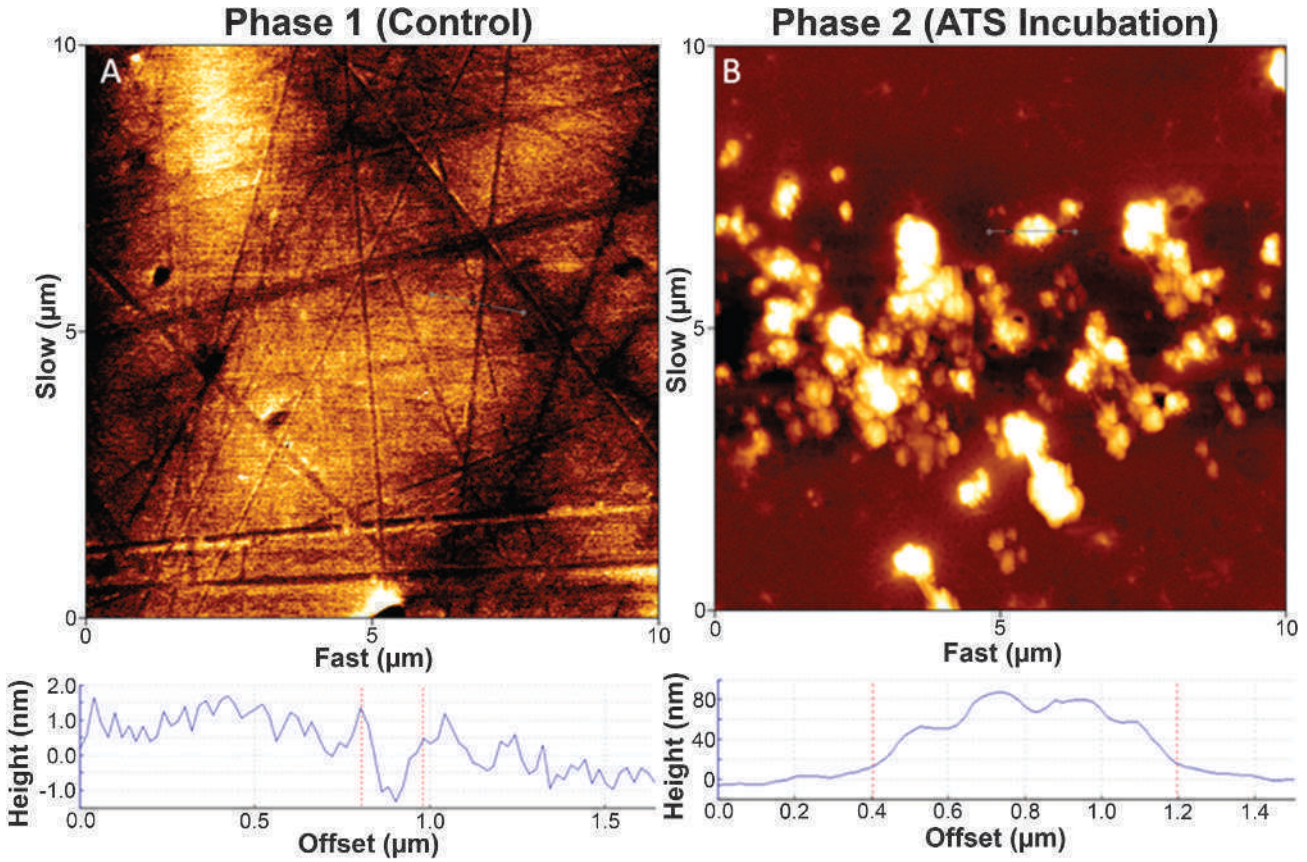

FIGURE 8.

Surface topography and cross section of LB before cleaning. Images were obtained using AFM. Beneath each image is its associated cross section displaying relative heights. (A) Control lens surface out of its blister package. (B) Lens surface after incubating in ATS for 1 week.

the macropores and silicate lines were no longer visible after incubating in ATS.

Figs. 3 and 4 illustrate the two independent cleaning pathways involving HPS and MPS, respectively. Fig. 3A (phase 3) reveals a relatively flat surface, exposing its macropores and silicate islands. The same phenomenon is seen in Fig. 4A (phase 3), although components of the MPS were adsorbed onto the surface as about 20-nm-high domains, specifically along the silicate lines. Fig. 4D (phase 6) is resolved and its surface exhibits a similar characteristic to that of Fig. 4A (phase 3), with features ranging between 15 and 20 nm in height. Likewise, Fig. 3D (phase 6) appears similar to Fig. 3A (phase 3).

Fig. 3B (phase 4) shows deposits ranging between 15 and 35 nm. However, Fig. 4B (phase 4) shows about 20-nm-high deposits scarcely across the surface. In addition, the macropores and silicate lines were clearly seen. Lastly, BA lenses in phase 5 with their respectful cleaning solution exhibited a similar surface to phase 3.

Senofilcon A

A 10- by 10-µm AFM scan of SA in phase 1 (A) and 2 (B) is shown in Fig. 5. The surface in phase 1 demonstrated a highly porous, ''spongelike'' appearance. These small pores were about 4 nm deep and uniformly present throughout the surface. Phase 2 contained extensive deposition that completely occluded the surface, with deposit heights up to 100 nm.

Figs. 6 and 7 illustrate the two independent cleaning pathways involving HPS and MPS, respectively. Fig. 6A (phase 3) reveals the porous nature of SA with small deposits. These deposits are also seen in Fig. 6D (phase 6), with heights ranging between 5 and 10 nm. Fig. 7A (phase 3) shows MPS components adsorbed, which completely covered the surface. These features appeared as about 5- to 10-nm-high domains with 15- to 30-nm-high deposits on top. Fig. 7D (phase 6) is resolved, and its surface also exhibits these features and heights, suggesting that it was derived from the MPS.

Fig. 6B (phase 4) presents a few deposits of heights up to 100 nm on the surface. In addition, the spongelike pores were also visible. Similarly, Fig. 7B (phase 4) had deposits ranging between 60 and 70 nm high across the surface with the spongelike pores visible, as well. However, most of the surface was covered by 10- to 20-nm-high domains. Lastly, SA lenses undergoing phase 5 with their respectful cleaning solution were similar to those undergoing phase 3.

Lotrafilcon B

A 10- by 10-µm AFM scan of LB in phase 1 (A) and 2 (B) is shown in Fig. 8. The surface of phase 1 was relatively flat, with lathe lines from the molds running in all directions on the surface. The surface topography of phase 2 yielded cluster of deposits as high as 90 nm, while leaving large regions free of deposition.

Figs. 9 and 10 illustrate the two independent cleaning pathways involving HPS and MPS, respectively. Fig. 9A (phase 3) reveals

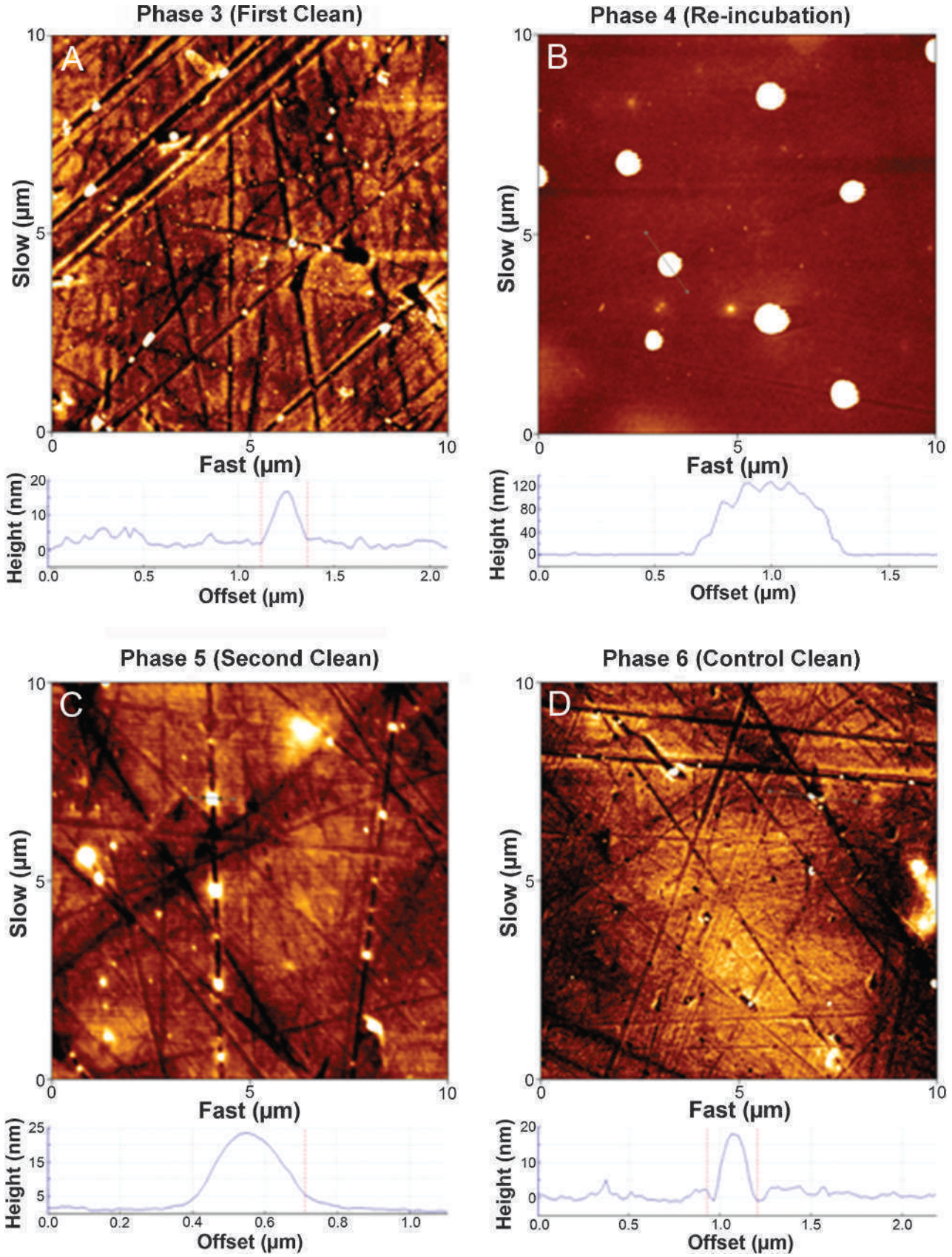

FIGURE 9.

Surface topography and cross section of LB with HPS cleaning. Images were obtained using AFM. Beneath each image is its associated cross section displaying relative heights. (A) Lens surface after first overnight clean with HPS. (B) HPS-cleaned lens surface after reincubating in ATS for 1 week. (C) Lens surface after second overnight clean with HPS. (D) Control lens surface cleaned with HPS.

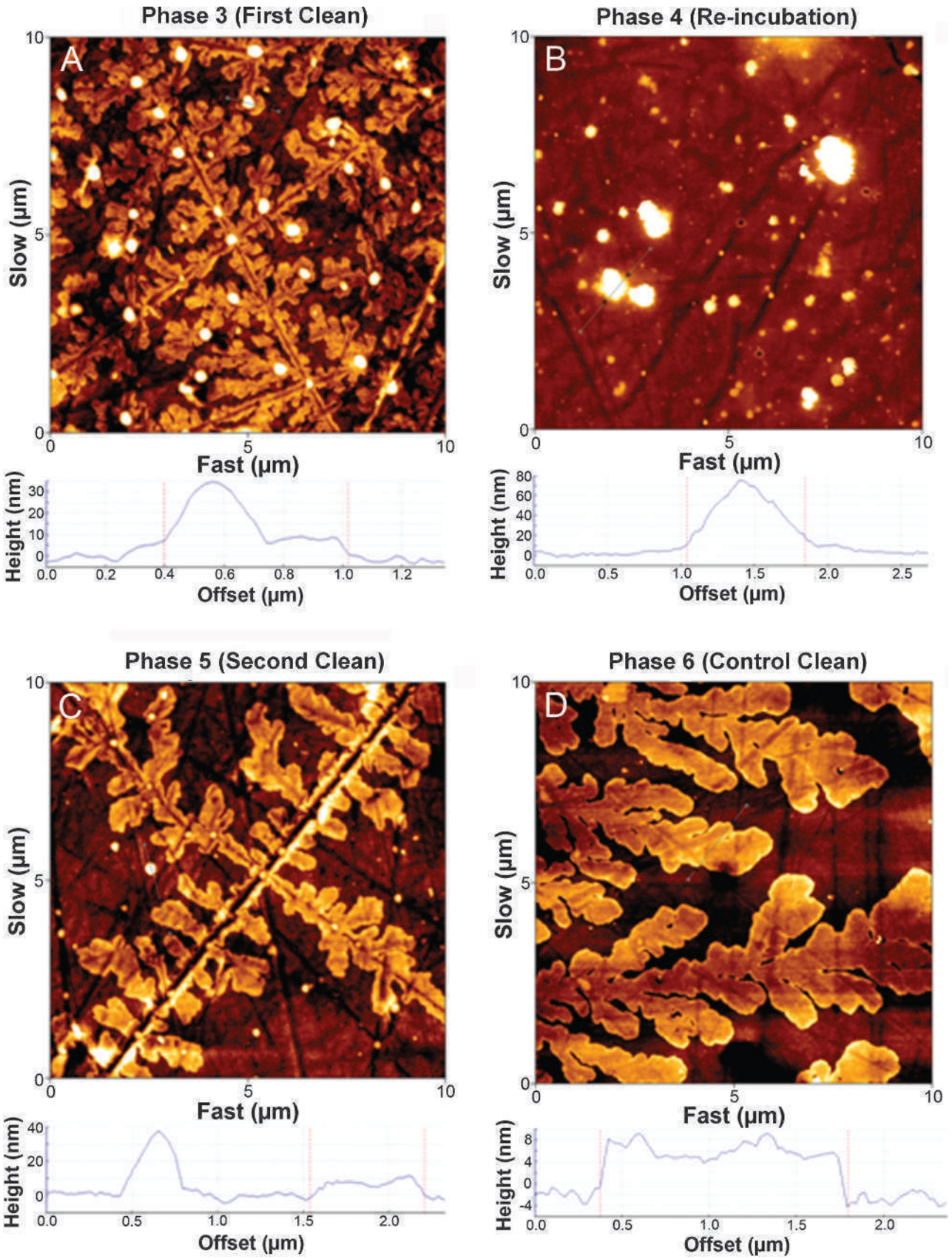

FIGURE 10.

Surface topography and cross section of LB with MPS cleaning. Images were obtained using AFM. Beneath each image is its associated cross section displaying relative heights. (A) Lens surface after first overnight clean with MPS. (B) MPS-cleaned lens surface after reincubating in ATS for 1 week. (C) Lens surface after second overnight clean with MPS. (D) Control lens surface cleaned with MPS.

TABLE 4.
Average surface roughness (R_a)

	R_a balafilcon A, nm		R_a senofilcon A, nm		R_a lotrafilcon B, nm	
	HPS	MPS	HPS	MPS	HPS	MPS
Phase 1	4.26 ± 1.58		1.65 ± 0.12		0.74 ± 0.13	
Phase 2	1.82 ± 0.40		36.92 ± 12.75		15.96 ± 7.21	
Phase 3	3.99 ± 1.14	5.75 ± 1.48	0.94 ± 0.12*	4.00 ± 0.89*	1.21 ± 0.15*	4.12 ± 0.65*
Phase 4	6.39 ± 2.59*	4.35 ± 0.96	5.31 ± 3.76*	7.23 ± 3.58*	8.28 ± 9.15*	10.14 ± 7.53*
Phase 5	4.54 ± 1.69	4.92 ± 1.28	1.32 ± 0.18	5.01 ± 0.92	1.10 ± 0.40	3.90 ± 0.64

*Significance ($p < 0.05$) compared to phase 2 for each respective lens material.

the randomly oriented lathe lines, as well as 15- to 20-nm deposits derived from the cleaning solution; these deposits are also seen in Fig. 9D (phase 6) with heights also ranging between 15 and 20 nm. Fig. 10A (phase 3) also reveals the lathe lines, but its surface showed MPS components adsorbed with heights up to 10 nm. Additionally, several 30- to 40-nm deposits were seen associated with the MPS residues, although they were absent in Fig. 10D (phase 6).

Fig. 9B (phase 4) reveals a few spaced-out deposits with heights of up to 140 nm. When examined closer, the lathe lines were faintly seen in the background. Similarly, Fig. 10B (phase 4) also contained deposits on the surface, though they were smaller with heights up to 80 nm. In addition, the lathe lines were more apparent and visible on the surface. Lastly, LB lenses undergoing phase 5 with their respectful cleaning solution were similar to those undergoing phase 3.

Average Surface Roughness

For each phase of the study, the average surface roughness (R_a) was generated using the JPK data processing software. This value represents the mean surface height of features above and below a central plane. The R_a values during each phase are shown in Table 4. For phase 1 lenses, BA exhibited the highest R_a value (4.26 ± 1.58 nm) and roughest surface compared with SA (1.65 ± 0.12 nm), whereas LB had the lowest R_a value (0.74 ± 0.13 nm). When cleaned with either HPS or MPS during phase 3, R_a values were smaller compared with phase 2 for SA and LB ($p < 0.05$). Similarly, both HPS- and MPS-phase 4 SA and LB lenses displayed a lower R_a compared with phase 2 lenses ($p < 0.05$).

There was no statistical significance in R_a between phase 2 BA lenses to HPS-phase 3 ($p = 0.96$) and MPS-phase 3 ($p = 0.08$) BA lenses. However, the HPS-phase 4 BA lens had a higher R_a compared with the phase 2 lens ($p < 0.05$), although no statistical significance was observed with MPS-phase 4 BA lens ($p = 0.83$). Additionally, there were no significant differences in R_a between HPS- and MPS-cleaned lenses for BA ($p > 0.98$), SA ($p > 0.48$), and LB ($p > 0.58$).

DISCUSSION

In this study, three different SH materials were investigated for their interaction with a well-characterized ATS and two different lens solutions: HPS and MPS. The three lens materials (BA, SA, and LB) were selected because each material has a different form of surface and/or wettability enhancement. There have been several studies that reported the use of AFM to image surface features and deposition morphologies of various contact lenses,[22,24,38–45] but none have used it to evaluate the efficacy of cleaning solutions. Atomic force microscopy is a powerful tool that can be used to assess the effectiveness of a cleaning solution on surfaces at the nanometer scale with high resolution.

Control lens images (Figs. 2A, 5A, and 8A for BA, SA, and LB, respectively) were obtained upon removing the lens from their packages. Significant differences in surface features were seen, which have been accredited to their specific modification process. Atomic force microscopy images of BA revealed their silicate islands and macropores and were consistent with other AFM studies.[22,24,42] Based on the cross section through a macropore, its depth measured about 20 nm. However, there has been speculation that these macropores are channels that penetrate the entire thickness of the lens,[21,24,42] although evidence from the cross section suggests otherwise. It is possible that the cantilever is limited to scanning pores deeper than 20 nm; therefore, further work should investigate the true depths of these macropores. Senofilcon A phase 1 images yielded a spongelike surface that is also consistent with previous AFM studies and is likely attributed to the unique incorporation of PVP to enhance wettability.[22] The numerous pores on the surface had a depth between 2 and 4 nm, which is significantly smaller than the macropores in BA. Images of LB phase 1 lenses also concurred with other AFM studies, with the presence of ''lathe lines'' on the surface.[48] Although these lines suggest that LB is manufactured through lathe-cut technology, this is not the case. Instead, these lenses are polymerized in cast molds containing lathe or polishing impressions that are transferred onto the lens surface.

Differences in ATS deposition in phase 2 were observed for all lens types, which were likely attributed to the specific surface treatment and material characteristics of each lens. The surface of SA exhibited relatively heavy ATS deposition (Fig. 5B), occluding the surface with heights greater than 100 nm. Conversely, the surface of BA contained uniformly smaller deposits that did not obstruct the surface (Fig. 2B). The AFM findings for these two lenses are not consistent with studies on lipid adsorption, because BA and SA have been shown to deposit relatively high levels of lipids.[10,49,50] One possible explanation for this discrepancy is that lipids, and proteins to a lesser extent, are being absorbed into the matrix of BA, whereas they are adsorbed and visible on the surface of SA. This claim is supported by the fact that BA is a negatively charged material and has significant absorptive capabilities, whereas SA is nonionic and not as absorptive.[51] Additionally, the macropores may serve as a desirable site for molecules to deposit into, as seen by the incubated lenses exhibiting

no sign of the macropores. For SA, the apparently large amount of deposition may be linked to its internal wetting agent, PVP. Despite being relatively hydrophilic, PVP is a polymer of *N*-vinyl pyrrolidone, which is known to be lipophilic and has been linked to increased lipid deposition.[52–55] What should be borne in mind is that the clinical relevance of this degree of apparent deposition remains unknown, and some degree of deposition may actually be beneficial in terms of the creation of a "biocompatible" surface. Indeed, previous work has suggested that the deposition of certain lipids may actually be helpful in lowering surface contact angle.[56]

The surface of LB exhibited an intermediate degree of deposition compared with BA and SA. These deposits appeared globular and clustered around other neighboring deposits, while leaving large areas vacant. Previous work with LB has shown it depositing the least of all SH lenses because of its plasma-coat treatment.[49,57,58] In addition, confocal laser scanning microscopy has shown that most constituents adsorb to the surface of the lens and do not penetrate into the matrix of the material.[58,59] Therefore, most of the deposits are bound onto the surface, which is confirmed in Fig. 8B. The globular nature of the deposits can be explained by already bound molecules on the surface serving as a foundation for more lipids and/or proteins to bind to, thus explaining the localization of these deposits.

Lenses cleaned with either the HPS or MPS regimen showed significant reduction in deposits on their surfaces. Specifically, AFM scans of all lenses that had been cleaned with HPS revealed a surface that was relatively similar to control lenses, suggesting that the surface was well cleaned by this solution. One observation with the HPS-cleaned lenses compared with their blister control is the presence of 15- to 20-nm-high circular deposits. These were also seen on the HPS clean control lens (phase 6), and it is possible that these deposits are derived from the Pluronic 17R4 surfactant in the HPS. They were seen on the surfaces of HPS-cleaned SA and LB, but not BA. As mentioned previously, it is possible that the surfactant was absorbed into the matrix of BA, while adsorbing onto the surface for the other two lens types.

The surface of all MPS-cleaned and MPS control lenses contained 10- to 15-nm-high domain-like residues, which are likely derived from components in the highly complex MPS (Table 1). On BA, these domains associated along the silicate lines, whereas they were more or less along the lathe lines on LB. The MPS interaction on SA adopted a different appearance, such that the domains appeared as islands occluding most of the surface with 20- to 30-nm-high deposits on them. Jacob et al.[60] measured the hydrophobicity of a commercial lens surface before and after cleaning with an MPS and found that surface hydrophobicity decreased after MPS cleaning. It is believed that the MPS blocked the hydrophobic surface domains, preventing biofouling of the lens via tear film deposition. This is evidently seen in BA, where the MPS associated along the silicate lines, which are relatively hydrophobic silicone portions on the polymer surface that have not been converted to silicate.[61]

In Figs. 3B and 4B, the surface after ATS reincubation for HPS- and MPS-cleaned BA is shown, respectively. When compared with the initial ATS incubation, the HPS did not appear to offer any surface protection against deposition, as large deposits were present. In comparison, the MPS appeared to have prevented the biofouling of the lens surface after reincubation, which was evident owing to the decreased density in deposits, as well as visibility of the silicate lines and macropores. Therefore, it is likely that the MPS residues on the lens blocked the hydrophobic domains and prevented further deposition on the surface.

Senofilcon A lenses in phase 4 revealed distinct differences compared with the heavily occluded surface seen in phase 2. Fig. 6B has a few large deposits of heights up to 100 nm; however, most of the surface was bare, as evidenced by the visibility of the spongelike pores. Fig. 7B also exhibits these pores, although most of the surface contained island-like domains, which resembled the MPS island-like domains described earlier. It is possible that the MPS components adsorbed tightly onto the surface, such that it manifested into a discontinuous coating.

In Fig. 9B, phase 4 LB lenses revealed a relatively flat surface containing a few localized deposits of heights up to 140 nm. Despite these deposits appearing larger compared with phase 2 in Fig. 8B, fewer were observed. Additionally, the lathe lines that are characteristic for LB were faintly seen, suggesting that the surface was not heavily occluded with tear film constituents because of HPS treatment. The surface in Fig. 10B also yielded a similar surface topography, although it contained smaller 80-nm-high deposits throughout the surface, and the lathe lines were more apparent. As mentioned with the other lens materials, it is likely that the MPS had a role in keeping the surface relatively resistant from ATS deposition.

Each lens material had a relatively low R_a value in their blister control, with BA greater than SA, and SA greater than LB, which concurs with several previous AFM studies.[22,24,42] Because R_a is calculated by drawing multiple cross sections on the surface, it is expected that BA would have the roughest surface owing to the macropores and discontinuous silicate islands. Similarly, SA contains pores on its surface that contributes to its roughness. Lotrafilcon B lenses exhibited the smoothest surface corresponding to a low R_a, which is likely attributed to its continuous surface coating.

R_a was also used to assess the efficacy of both cleaning solutions quantitatively. It was shown that the R_a did not differ significantly between lenses that were cleaned with HPS to those cleaned with MPS. For both SA and LB, a significant reduction in R_a was seen after cleaning with HPS and MPS. This was also evident in the AFM images, as cleaning removed most tear film deposits, thus producing control-like surfaces. Furthermore, the R_a of phase 4 lenses was significantly less than the R_a in phase 2. It has been proposed, and evidently seen in the results, that a lens regimen can affect the way tear constituents deposit onto the surface.[62–64] Therefore, this is further evidence supporting the supposition that both lens solutions provide some form of resistance to surface deposition.

Despite AFM images revealing the impact that both HPS and MPS have on cleaning the surface of BA, there was no statistical significance in R_a between phase 2 and 3 lenses. In addition, phase 4 lenses cleaned with HPS showed a significant increase in R_a compared with phase 2, whereas phase 4 lenses that were cleaned with MPS showed no difference in R_a. These results suggest that both cleaning regimens fail to completely clean the surface and provide some form of deposition resistance. However, given that R_a measurements are calculated by averaging multiple cross sections on the surface, these values can vary immensely for BA owing to the presence of the macropores. If a random cross section was drawn through a macropore, it would cause the R_a to be much greater than a cross section that was not. Therefore, R_a measurements on BA are not an accurate indication of cleaning

solution efficiency because both a clean and soiled surface can result in a large R_a.

Although imaging with AFM provides tremendous advantages and helps to resolve the morphology of lens deposits with high resolution, the results obtained from this study should be carefully interpreted. The reason for this is that the lens is at risk of dehydrating from imaging in air, which is not representative of a lens on the ocular surface, because tears constantly hydrate the lens to maintain a moist environment. Furthermore, the state of the deposits on the lens surface may alter when exposed to air, such as leeching back into the lens matrix. However, this was an exploratory study to see whether AFM was capable of imaging lenses treated with cleaning solution, which was shown to be successful. Imaging in a liquid environment was difficult to achieve because of the curved surface of the lens and difficulties in lens attachment on the substrate, which was why lenses were imaged in air. Regardless of the medium, a potential confounding factor to consider is the area being scanned, because it is difficult at the micrometer scale to scan the exact central location between different treated lenses. To circumvent this issue, the AFM stage was fixed so that the area being scanned was relatively consistent to minimize any potential bias during analysis. Another limitation is that AFM imaging is restricted to surface topography and gives no insight regarding the inside of the material. Furthermore, any proposed clinical relationship between these visible domains and in-eye comfort should be cautiously interpreted. Future work may include using AFM in a force measurements regimen, to measure the adhesion forces or investigate the effects these cleaning regimens have on the matrix of the lens using confocal laser scanning microscopy. Nonetheless, these findings do provide a foundation for examining contact lenses at the nanometer scale.

CONCLUSIONS

Specific surface features of each of the SH lenses were observed using AFM and how they interacted with an ATS. In addition, the efficacy of an HPS and MPS cleaning regimen was assessed, where both displayed significant removal of surface deposits, although there were no significant differences in surface roughness after cleaning between the two solutions. Although surface roughness is one measure of cleaning efficacy, it does not fully describe the overall process that takes place on the lens surface. To supplement, the qualitative data from the AFM images provide some insight regarding the potential cleaning process occurring. For instance, the use of an MPS and HPS leaves behind residues onto the lens surface, which may initially appear as having a positive effect by the reduction in surface deposits. Future work should examine these cleaning solution components and their interaction with the lens and ocular surface.

ACKNOWLEDGMENTS

The authors thank Sarah Hagedorn, BSc, at the University of Waterloo School of Optometry and Vision Science, for developing the spherical glass to mount the contact lens for AFM imaging and Dr. Ravi Gaikwad (PhD) for AFM training and assistance.

This study was sponsored by the Natural Sciences and Engineering Research Council of Canada. The AFM infrastructure was supported by the Canadian Foundation for Innovation, Ontario Research Fund, and the University of Waterloo.

One of the authors (LWJ) has received funding from the following companies who are directly involved in the manufacture of competing products: Abbott Medical Optics, Advanced Vision Research, Alcon, AlgiPharma, Allergan, Bausch + Lomb, CIBA Vision, CooperVision, Essilor, Johnson & Johnson Vision Care, Oculus, TearScience, and Visioneering Technologies.

Received January 8, 2014; accepted June 23, 2014.

REFERENCES

1. Morgan PB, Efron N, Helland M, Itoi M, Jones D, Nichols JJ, van der Worp E, Woods CA. Twenty first century trends in silicone hydrogel contact lens fitting: an international perspective. Cont Lens Anterior Eye 2010;33:196–8.
2. Jalbert I, Stretton S, Naduvilath T, Holden B, Keay L, Sweeney D. Changes in myopia with low-Dk hydrogel and high-Dk silicone hydrogel extended wear. Optom Vis Sci 2004;81:591–6.
3. Alvord L, Court J, Davis T, Morgan CF, Schindhelm K, Vogt J, Winterton L. Oxygen permeability of a new type of high Dk soft contact lens material. Optom Vis Sci 1998;75:30–6.
4. Compan V, Andrio A, Lopez-Alemany A, Riande E, Refojo MF. Oxygen permeability of hydrogel contact lenses with organosilicon moieties. Biomaterials 2002;23:2767–72.
5. Efron N, Morgan PB, Cameron ID, Brennan NA, Goodwin M. Oxygen permeability and water content of silicone hydrogel contact lens materials. Optom Vis Sci 2007;84:328–37.
6. Tighe BJ. A decade of silicone hydrogel development: surface properties, mechanical properties, and ocular compatibility. Eye Contact Lens 2013;39:4–12.
7. Tighe B. Silicone hydrogels: structure, properties and behaviour. In: Sweeney D, ed. Silicone Hydrogels: Continuous Wear Contact Lenses, Oxford: Butterworth-Heinemann, 2004:1–27.
8. Nichols JJ. Deposition on silicone hydrogel lenses. Eye Contact Lens 2013;39:20–3.
9. Pucker AD, Thangavelu M, Nichols JJ. In vitro lipid deposition on hydrogel and silicone hydrogel contact lenses. Invest Ophthalmol Vis Sci 2010;51:6334–40.
10. Lorentz H, Heynen M, Trieu D, Hagedorn SJ, Jones L. The impact of tear film components on in vitro lipid uptake. Optom Vis Sci 2012;89:856–67.
11. Lorentz H, Jones L. Lipid deposition on hydrogel contact lenses: how history can help us today. Optom Vis Sci 2007;84:286–95.
12. Subbaraman LN, Jones L. Kinetics of lysozyme activity recovered from conventional and silicone hydrogel contact lens materials. J Biomater Sci Polym Ed 2010;21:343–58.
13. Subbaraman LN, Glasier MA, Senchyna M, Sheardown H, Jones L. Kinetics of in vitro lysozyme deposition on silicone hydrogel, PMMA, and FDA groups I, II, and IV contact lens materials. Curr Eye Res 2006;31:787–96.
14. Suwala M, Glasier MA, Subbaraman LN, Jones L. Quantity and conformation of lysozyme deposited on conventional and silicone hydrogel contact lens materials using an in vitro model. Eye Contact Lens 2007;33:138–43.
15. Jones L, Senchyna M, Glasier MA, Schickler J, Forbes I, Louie D, May C. Lysozyme and lipid deposition on silicone hydrogel contact lens materials. Eye Contact Lens 2003;29:S75–9.
16. Senchyna M, Jones L, Louie D, May C, Forbes I, Glasier MA. Quantitative and conformational characterization of lysozyme deposited on balafilcon and etafilcon contact lens materials. Curr Eye Res 2004; 28:25–36.

17. Luensmann D, Jones L. Protein deposition on contact lenses: the past, the present, and the future. Cont Lens Anterior Eye 2012; 35:53–64.
18. Fonn D, Dumbleton K. Dryness and discomfort with silicone hydrogel contact lenses. Eye Contact Lens 2003;29:S101–4.
19. Fonn D. Targeting contact lens induced dryness and discomfort: what properties will make lenses more comfortable. Optom Vis Sci 2007;84:279–85.
20. Tighe B. Silicone hydrogel materials: how do they work? In: Sweeney DF, ed. Silicone Hydrogels: The Rebirth of Continuous Wear Contact Lenses, Oxford: Butterworth Heinemann, 2000:1–21.
21. Lopez-Alemany A, Compan V, Refojo MF. Porous structure of Purevision versus Focus Night&Day and conventional hydrogel contact lenses. J Biomed Mater Res 2002;63:319–25.
22. Teichroeb JH, Forrest JA, Ngai V, Martin JW, Jones L, Medley J. Imaging protein deposits on contact lens materials. Optom Vis Sci 2008;85:1151–64.
23. Weikart CM, Matsuzawa Y, Winterton L, Yasuda HK. Evaluation of plasma polymer-coated contact lenses by electrochemical impedance spectroscopy. J Biomed Mater Res 2001;54:597–607.
24. Gonzalez-Meijome JM, Lopez-Alemany A, Almeida JB, Parafita MA, Refojo MF. Microscopic observation of unworn siloxane-hydrogel soft contact lenses by atomic force microscopy. J Biomed Mater Res B Appl Biomater 2006;76:412–8.
25. Steffen R, Schnider C. A next generation silicone hydrogel lens for daily wear. Part 1—material properties. Optician 2004;227:23–5.
26. Morgan PB, Efron N. A decade of contact lens prescribing trends in the United Kingdom (1996–2005). Cont Lens Anterior Eye 2006; 29:59–68.
27. Dalton K, Subbaraman LN, Rogers R, Jones L. Physical properties of soft contact lens solutions. Optom Vis Sci 2008;85:122–8.
28. Jones L, Senchyna M. Soft contact lens solutions review: part 1—components of modern care regimens. Optom Pract 2007;8:45–56.
29. Mok KH, Cheung RW, Wong BK, Yip KK, Lee VW. Effectiveness of no-rub contact lens cleaning on protein removal: a pilot study. Optom Vis Sci 2004;81:468–70.
30. Franklin VJ. Cleaning efficacy of single-purpose surfactant cleaners and multi-purpose solutions. Cont Lens Anterior Eye 1997;20:63–8.
31. Zhu H, Bandara MB, Vijay AK, Masoudi S, Wu D, Willcox MD. Importance of rub and rinse in use of multipurpose contact lens solution. Optom Vis Sci 2011;88:967–72.
32. Cho P, Cheng SY, Chan WY, Yip WK. Soft contact lens cleaning: rub or no-rub? Ophthalmic Physiol Opt 2009;29:49–57.
33. Rosenthal RA, Henry CL, Stone RP, Schlech BA. Anatomy of a regimen: consideration of multipurpose solutions during non-compliant use. Cont Lens Anterior Eye 2003;26:17–26.
34. Pucker AD, Nichols JJ. Impact of a rinse step on protein removal from silicone hydrogel contact lenses. Optom Vis Sci 2009;86:943–7.
35. Butcko V, McMahon TT, Joslin CE, Jones L. Microbial keratitis and the role of rub and rinsing. Eye Contact Lens 2007;33:421–3.
36. Kilvington S, Lonnen J. A comparison of regimen methods for the removal and inactivation of bacteria, fungi and *Acanthamoeba* from two types of silicone hydrogel lenses. Cont Lens Anterior Eye 2009;32:73–7.
37. Last JA, Russell P, Nealey PF, Murphy CJ. The applications of atomic force microscopy to vision science. Invest Ophthalmol Vis Sci 2010;51:6083–94.
38. Giraldez MJ, Serra C, Lira M, Real Oliveira ME, Yebra-Pimentel E. Soft contact lens surface profile by atomic force microscopy. Optom Vis Sci 2010;87:475–81.
39. Lira M, Santos L, Azeredo J, Yebra-Pimentel E, Oliveira ME. Comparative study of silicone-hydrogel contact lenses surfaces before and after wear using atomic force microscopy. J Biomed Mater Res B Appl Biomater 2008;85:361–7.
40. Guryca V, Hobzova R, Pradny M, Sirc J, Michalek J. Surface morphology of contact lenses probed with microscopy techniques. Cont Lens Anterior Eye 2007;30:215–22.
41. Kim SH, Opdahl A, Marmo C, Somorjai GA. AFM and SFG studies of pHEMA-based hydrogel contact lens surfaces in saline solution: adhesion, friction, and the presence of non-crosslinked polymer chains at the surface. Biomaterials 2002;23:1657–66.
42. Gonzalez-Meijome JM, Lopez-Alemany A, Almeida JB, Parafita MA. Surface AFM microscopy of unworn and worn samples of silicone hydrogel contact lenses. J Biomed Mater Res B Appl Biomater 2009;88:75–82.
43. Baguet J, Sommer F, Claudon-Eyl V, Duc TM. Characterization of lacrymal component accumulation on worn soft contact lens surfaces by atomic force microscopy. Biomaterials 1995;16:3–9.
44. Baguet J, Sommer F, Duc TM. Imaging surfaces of hydrophilic contact lenses with the atomic force microscope. Biomaterials 1993; 14:279–84.
45. Bhatia S, Goldberg EP, Enns JB. Examination of contact lens surfaces by Atomic Force Microscope (AFM). CLAO J 1997;23:264–9.
46. Lorentz H, Heynen M, Kay LM, Dominici CY, Khan W, Ng WW, Jones L. Contact lens physical properties and lipid deposition in a novel characterized artificial tear solution. Mol Vis 2011;17: 3392–405.
47. Lorentz H, Heynen M, Tran H, Jones L. Using an in vitro model of lipid deposition to assess the efficiency of hydrogen peroxide solutions to remove lipid from various contact lens materials. Curr Eye Res 2012;37:777–86.
48. Subbaraman LN, Woods J, Teichroeb JH, Jones L. Protein deposition on a lathe-cut silicone hydrogel contact lens material. Optom Vis Sci 2009;86:244–50.
49. Carney FP, Nash WL, Sentell KB. The adsorption of major tear film lipids in vitro to various silicone hydrogels over time. Invest Ophthalmol Vis Sci 2008;49:120–4.
50. Pitt WG, Perez KX, Tam NK, Handly E, Chinn JA, Liu XM, Maziarz EP. Quantitation of cholesterol and phospholipid sorption on silicone hydrogel contact lenses. J Biomed Mater Res B Appl Biomater 2013;101:1516–23.
51. Boone A, Heynen M, Joyce E, Varikooty J, Jones L. Ex vivo protein deposition on bi-weekly silicone hydrogel contact lenses. Optom Vis Sci 2009;86:1241–9.
52. Jones L, Evans K, Sariri R, Franklin V, Tighe B. Lipid and protein deposition of *N*-vinyl pyrrolidone-containing group II and group IV frequent replacement contact lenses. CLAO J 1997;23:122–6.
53. Jones L, Mann A, Evans K, Franklin V, Tighe B. An in vivo comparison of the kinetics of protein and lipid deposition on group II and group IV frequent-replacement contact lenses. Optom Vis Sci 2000;77:503–10.
54. Bontempo AR, Rapp J. Protein-lipid interaction on the surface of a hydrophilic contact lens in vitro. Curr Eye Res 1997;16:776–81.
55. Bontempo AR, Rapp J. Protein-lipid interaction on the surface of a rigid gas-permeable contact lens in vitro. Curr Eye Res 1997; 16:1258–62.
56. Lorentz H, Rogers R, Jones L. The impact of lipid on contact angle wettability. Optom Vis Sci 2007;84:946–53.
57. Lorentz H, Heynen M, Khan W, Trieu D, Jones L. The impact of intermittent air exposure on lipid deposition. Optom Vis Sci 2012;89:1574–81.

58. Luensmann D, Glasier MA, Zhang F, Bantseev V, Simpson T, Jones L. Confocal microscopy and albumin penetration into contact lenses. Optom Vis Sci 2007;84:839–47.
59. Luensmann D, Zhang F, Subbaraman L, Sheardown H, Jones L. Localization of lysozyme sorption to conventional and silicone hydrogel contact lenses using confocal microscopy. Curr Eye Res 2009;34:683–97.
60. Jacob JT, Levet J, Jr, Edwards TA, Dassanayake N, Ketelson H. Visualizing hydrophobic domains in silicone hydrogel lenses with Sudan IV. Invest Ophthalmol Vis Sci 2012;53:3473–80.
61. Jones L, Dumbleton K. Silicone hydrogel contact lenses: part 1—evolution and current status. Optom Today 2002;20:26–31.
62. Nichols JJ. Deposition rates and lens care influence on galyfilcon A silicone hydrogel lenses. Optom Vis Sci 2006;83:751–7.
63. Lebow KE, Christensen B. Cleaning efficacy and patient comfort: a clinical comparison of two contact lens care systems. Int Contact Lens Clin 1996;23:87–93.
64. Omali NB, Zhao Z, Zhong L, Raftery MJ, Zhu H, Ozkan J, Willcox M. Quantification of protein deposits on silicone hydrogel materials using stable-isotopic labeling and multiple reaction monitoring. Biofouling 2012;28:697–709.

Steven Cheung
School of Optometry and Vision Science
University of Waterloo
200 University Avenue W
Waterloo, Ontario, N2L 3G1
Canada
e-mail: s4cheung@uwaterloo.ca